Journal of Advances in Medical and Pharmaceutical Sciences
5(4): 1-16, 2016, Article no.JAMPS.22134
ISSN: 2394-1111

SCIENCEDOMAIN *international*
www.sciencedomain.org

MicroRNA Memory I: The Positive Correlation between Synergistic Effects of MicroRNAs in Cancer and a Novel Quantum Scoring System

Masaru Yoshikawa[1*], Tatsunori Osone[1] and Yoichi Robertus Fujii[1,2*]

[1]Nagoya City University, Pharmaco-MicroRNA Genomics, Graduate School of Pharmaceutical Sciences, Advanced Pharmaceutical Science Center, Nagoya, 467-8603, Japan.
[2]Nagoya City University, Retroviral Genetics Group, Graduate School of Pharmaceutical Sciences, Advanced Pharmaceutical Science Center, Nagoya, 467-8603, Japan.

Authors' contributions

This work was carried out in collaboration among all authors. Author MY wrote the protocol, performed the statistical analysis, drafted the manuscript, and did the literature search. Author TO collected all necessary sequence data. Author YRF designed and supervised the study. All authors read and approved the final manuscript.

Article Information

DOI: 10.9734/JAMPS/2016/22134
Editor(s):
(1) Faiyaz Shakeel, Department of Pharmaceutics, King Saud University, Riyadh, Saudi Arabia.
Reviewers:
(1) Kuan-Chih Chow, National Chung Hsing University, Taichung, Taiwan.
(2) Neamat Hanafi Ahmed Osman, National Centre for Radiation Research and Technology, Egypt.
(3) Martha E. Ruiz Tachiquin, Medical Research Unit In Human Genetics, IMSS, Mexico.
Complete Peer review History: http://sciencedomain.org/review-history/12414

Original Research Article

Received 19th September 2015
Accepted 9th November 2015
Published 24th November 2015

ABSTRACT

Aim: To investigate quantum characters of the microRNA (miRNA) gene as the disease memory device, at the beginning, a novel quantum scoring method was developed and its usability was confirmed by valuating miRNA–miRNA interaction.
Background: In general, activated miRNAs participate in regulation of gene expression via mainly inhibiting translation of messenger RNAs (mRNAs) into proteins. miRNAs select their target mRNAs by the degree of sequence complementarity between miRNAs and target sites on mRNA. Therefore, a precious prediction of miRNA–mRNA interaction would be useful for clear up miRNA–protein functions in biological processes. However, although many computer algorisms for miRNA target prediction have been developed and improved, they still have shown many incorrect results.

**Corresponding author: E-mail: c142637@ed.nagoya-cu.ac.jp, fatfuji@hotmail.co.jp;*

Thus, much more precise prediction tool *in silico* by using computers and databases is necessary.
Methods: First, the miRNA–miRNA synergism was investigated according to modified previous algorism, and some synergistically-working miRNA pairs were collected. Next, we developed two new quantum scores, Static Nexus Score (SNS) and then Dynamic Nexus Score (DNS), and calculated them for each synergistic miRNA pair. SNS and DNS were derived from the miRNA-miRNA matrix that calculates quantum interaction between miRNAs from quantum energy in each single miRNA nucleotide. The synergistic activities of the miRNA functional pairs were evaluated upon the fold changes as synergistic effect (SE).
Results: The relation of SE in miRNA functional activity was subsequently examined with DNSs. As a result, positive correlation (R = 0.55, $P < .06$) was observed between DNS and strength of SE of each synergistic miRNA pair which is related to oncogenesis or tumor suppression.
Conclusions: The single miRNA-miRNA synergism would be important to predict biological function of miRNAs in cancer. This is the first report arguing that miRNA synergism could be showed through calculating DNS of each miRNA pair as miRNA memory device.

Keywords: MicroRNA (miRNA); noncoding RNA; algorism; quantum; synergism; cancer.

ABBREVIATIONS

SE	*Synergistic Effect*
SNS	*Static Nexus Score*
DNS	*Dynamic Nexus Score*
TSS	*Transcription Start Site*
FMO	*Fragment Molecular Orbital method*

1. INTRODUCTION

MicroRNAs (miRNAs), which are approximately 20 nucleotides long, belong to the small non-coding RNAs [1]. These RNAs were once considered RNA fragments, but it has recently been revealed that miRNAs are gene, which is able to regulate biological processes in humans and other species, such as cell cycle, apoptosis, cell proliferation, immunoreaction, and tumorigenesis [2–7]. The functional miRNA complex is composed of the Argonaute protein binding to both the mRNA and miRNA, and this complex is able to suppress gene expression post-transcriptionally [8,9]. However, *in vivo* and *in vitro* experiments demonstrated that certain miRNAs may augment gene expression [10]. Individual miRNAs can interact with hundreds of mRNAs, and a single mRNA is controlled by numerous miRNAs; however, the binding affinity is different between each miRNA and mRNA [3,11,12]. Although interactions between miRNA and mRNA can be predicted using the seed theory-based algorithm, *in vitro* or *in vivo* experiments is not always confirmed by the predicted binding [13].

Web services and databases based on seed theory algorithms are available for miRNA target prediction, and these tools enable the comparison of results calculated with various algorithms (Table 1). For instance, the TargetScan, miRanda (miRBase), and miRDB systems are based on sequence complementarity between the miRNA seed region and target site in the mRNA [14–16]. DIANA-microT and PicTar use thermodynamics to calculate the stability or free energy of the miRNA–mRNA complex, and RNAhybrid utilizes both a statistical model and thermodynamics for prediction [15–18]. However, these target prediction systems suggest many incorrect candidates such as false positive and incorrect targets [13,19].

Original scores are now filtered, thus improving the results of prediction tools (Table 1). However, predictions investigating a one-to-one interaction between a miRNA seed and an mRNA target cannot predict multiple interactions of miRNAs and mRNAs. Therefore, high quality predictions cannot be obtained by improving the filtering alone.

Synergies between miRNAs regulate miRNA–mRNA interactions, and in numerous cases, these collaborations caused a more profound effect compared with that caused by a single miRNA [20,21]. miRNA–miRNA synergies may have a key function in regulating biological processes because they have potential to reveal the unexplainable target selection mechanisms, such as non-canonical and cell-specific targeting. Indeed, it is reported that interactions between miRNAs have been observed not only in co-target relations but also in multiple mode of function [22]. This suggests that there is room for allowing existence of miRNA–miRNA synergies. Therefore, to improve miRNA target prediction, scoring of miRNA–miRNA interactions would be beneficial, which has been reported in only a few publications [23].

Table 1. Existing target prediction services for miRNA

Service name	Base algorism	Filtering option	References
TargetScan	seed complementarity	conservation, target site abundance	[15,16]
miRanda	complementarity	thermodynamics	[15,16]
miRDB	support vector machine	conservation, expression profile, functional annotation	[14-16]
DIANA-microT	thermodynamics	seed complementarity, conservation, target site abundance	[15-17]
PicTar	thermodynamics	complementarity, co-expression, cross-species comparison	[15,16]
RNAhybrid	thermodynamics	statistical model	[16,18]

In our previous study, to elucidate miRNA biological functions at the nucleotide level, we developed an RNA wave model and annotated the RNA sequences using quantum theory and electrostatic potential according to RNA bases [24,25]. We constructed a matrix for simulating quantum interaction between RNAs and subsequently showed that a miRNA can transform the binary notation with qubit, and miRNA–viral RNA complexes can be expressed using the matrix [26]. Here, we introduce a novel quantum scoring method based on the quantum computing algorithm to investigate single miRNA–miRNA interactions. Using this technique, we found a positive correlation between quantum scoring and synergistic effects (SEs) of miRNAs in malignant diseases. Finally, we discuss the benefits of quantum scores in disease prediction, and in interpretation of microRNA as memory device. The G-based quantum superposition and entanglement of miRNAs could record, transmit, and even inherit biological statuses in cells, like memory devices in computers [25].

2. MATERIALS AND METHODS

2.1 microRNA Sequence Data

Sequences of mature miRNAs were downloaded as microRNA.dat and mature.fa from miRBase [27]. This data was Release 21 (date: June 2014) and the database contained 28,645 of all mature miRNA sequences. We extracted 2,588, 1,915, 466, 434, and 427 of human, murine, Drosophila, C. *elegans* and Arabidopsis mature miRNA sequences from above mature miRNAs, respectively.

2.2 Conversion of Sequence

All miRNA sequences downloaded from miRBase were converted into respective binary codes (ket alignments). According to the previous report, electrical potential of four basic nucleobases in RNA (Guanine, Adenine, Cytosine, and Uracil) were calculated by referring to FMO of each atom in nucleobase and by integrating them with quantum entanglement [24]. As a result, only G showed positive numeric value and the others showed negative ones, therefore, to consider about the basis state of spanning sets of bits in vector subspace of miRNA-FMOs, the binary transformation was performed into the state 1 and 0. G was transformed as 1 and the rest, U, A, and C as 0 [24].

2.3 The Quantum Matrix Construction

The matrix for quantum computation was made with Microsoft Office Excel 2013 (Microsoft Japan Co., Ltd., Tokyo, Japan) using its macro and function systems. The matrix is comprised of three parts; the upper part for loading miRNA pair sequences, the left and lower parts for arranging sequences, and the central part for calculating miRNA–miRNA interactions (Fig. 1). miRNA sequences set in the upper part will be loaded into the left and lower parts with the windows of 3 nucleotides, then interactions between each nucleotide and each its opposite nucleotide will be calculated at corresponded intersecting points on the central part. Although the relation of nucleobase binding is flexible phenomenon which occur in sufficiently tiny environments, we have previously reported the existence of quantum energy between or among miRNAs [24–26]. Original sequences of miRNAs are translated by binary notation based on the quantum energy of nucleotide (Fig. 1A), set in upper part of the matrix (Fig. 1C), and loaded into left and lower parts of matrix separately by the rule shown in Fig. 1B. Then matrix calculated and visualized the quantum state

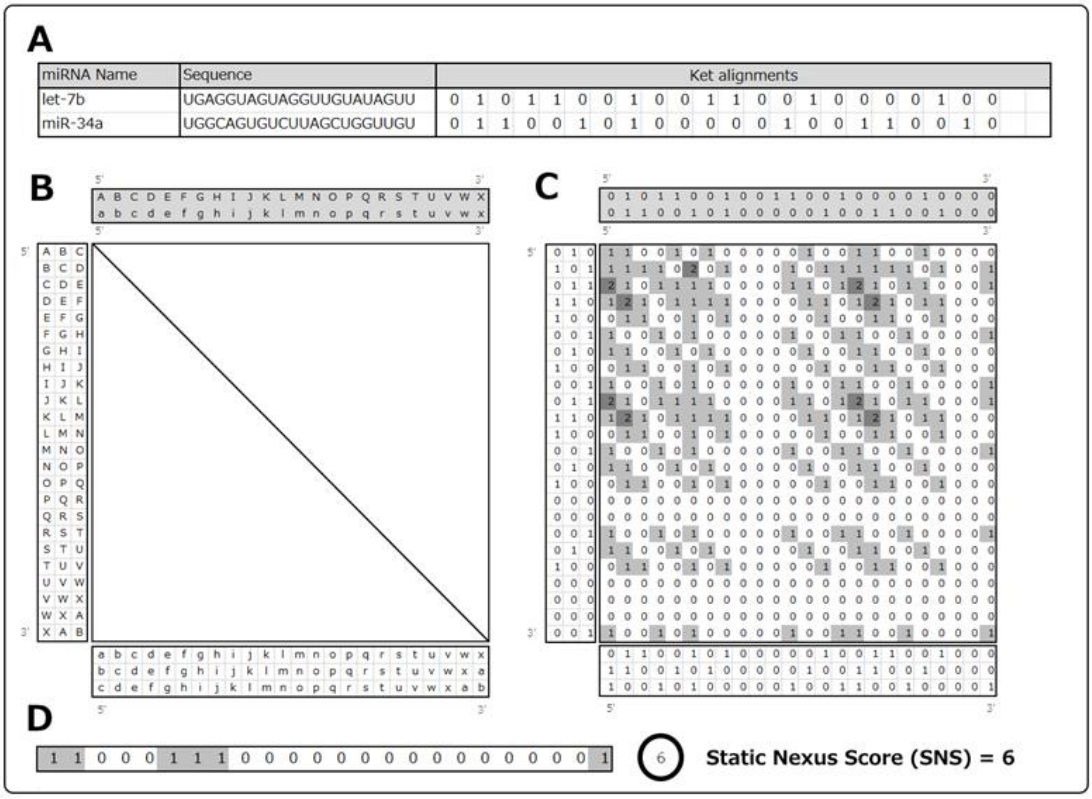

Fig. 1. The matrix for quantum calculation

between coupled miRNAs (Fig. 1C). The matrix architecture is derived from analogy of quantum computation [28].

2.4 The Quantum Calculation

Since information is physics and the miRNA gene is information, we here selected the matrix as the Hilbert space, which is a vector space possessing the structure of an inner product, of the Tensor products. The ket modules of two miRNAs in matrix, for instance, A and B are expressed as follows

$$z(|A> \otimes |B>) = (z|A> \otimes |B>) = (|A> \otimes z|B>) \quad (1, 0)$$

$$(a \otimes b)(|A> \otimes |B>) = a|A> \otimes b|B> \quad (1, 1)$$

From (1, 0) and (1, 1), $A \otimes B$ of the inner product spaces are represented the vector space of an intersecting point between |A> and |B> in the matrix.

$$(\sum a_i|A> \otimes B_i>, \sum b_j|A_j> \otimes |B_j>) \equiv \sum a_i * B_j < A_i|A_j >< B_i|B_j > \quad (1, 2)$$

Since RNA quantum code with the fragment molecular orbital method (FMO) of two miRNAs were calculated according to the binary notation of electro spin as previously described [24]. From (1, 2), miRNA–miRNA interaction was calculated in the matrix as a vector space. The coherent of sample miRNA values are applied into a matrix in the order with both rows and columns. When the f(x) is register y for a miRNA and the register x is the other miRNA the values of superpose samples are shown as amplitude vectors of an intersecting point between |x> and f(x) in the matrix. These calculation were performed by the original macro program, MESer [29]. An integer of the amplitude vectors, each superposition (SP) in the intersecting points on the decreasing diagonal of the matrix (1, 3) was summed up as Static Nexus Score (SNS) (1, 4).

$$\mathrm{SP_i} = \sum_{j=0}^{2} (A_{i+j} \times B_{i+j}) \quad (1, 3)$$

$$\mathrm{SNS} = 3 \times \sum_{i=0}^{23} (A_i \times B_i) \quad (1, 4)$$

The RNA wave model 2000 was based on circular miRNA electron spin, therefore two sample miRNAs were moving and shifting one by one and in the counter direction of each other [24–26]. Since the torus miRNAs can revolve in the matrix, SNS between two torus miRNAs (A_i, B_j) usually showed different values in each relative location shifting. Subsequently, they were summed up as Dynamic Nexus Score (DNS) for further experiments (i = 0, …, 23; j = 0, …, 23) (1, 5).

$$\mathrm{DNS} = 3 \times \sum_{i=0}^{23}\left(A_i \times \sum_{j=0}^{23} B_j\right) = 3 \times \sum_{i=0}^{23} A_i \times \sum_{j=0}^{23} B_j \quad (1, 5)$$

In the case of different nucleotide length of two miRNAs, the surplus space of 3' end region of miRNA was filled up with zeros.

2.5 Evaluation of Synergistic Effects of miRNAs

The biological activity of synergistic effects was investigated from previous reports about miRNA synergism. When a specific numerical value was shown in above reports as miRNA synergism, we directly applied the specific value to the comparison to the miRNA-miRNA quantum scores. Otherwise, the single miRNA activity unit (E) and synergistic miRNA activity unit (S) were calculated as follows,

$$\text{Single microRNA activity unit (E)} = \frac{\text{The single miRNA activity}}{\text{Total amounts of single miRNA}}$$

$$\text{Synergistic microRNA activity unit (S)} = \frac{\text{The synergistic miRNA activity}}{\text{Total amounts of synergitic miRNA}}$$

Total amounts mean an amount of miRNA that is applied to sample in each research, such as ng and mol.

A synergistic effect (SE) between $miRNA_a$ and $miRNA_b$ was calculated as follows,

$$\text{Synergistic Effect (SE)} = \frac{\text{S of miRNA}_\text{a} \text{ and miRNA}_\text{b}}{\text{E of miRNA}_\text{a} + \text{E}'\text{of miRNA}_\text{b}}$$

When a single miRNA pair has multiple synergistic activities, these synergistic effects were averaged as multiple SE unit (SEU) (i = 1, 2…, n),

$$\text{Multiple SE unit (SEU)} = \frac{\sum_\text{i}^\text{n} \text{SE}}{\text{n}}$$

3. RESULTS

3.1 MicroRNAs with the Binary Quantum Code

According to a previous report that compared electrical states among the four types of nucleic acid bases, only G has a positive electrical potential; the others have a negative one. We performed a new RNA evaluation by transforming the original RNA sequences into binary codes substituting Gs with 1 and the others with 0. Using this quantum theory, we transformed the hsa-let-7b and hsa-miR-34a miRNA sequences into a quantum code as a sample and defined these quantum codes as ket alignment according to the quantum mechanics field. Ket alignments of hsa-let-7b and hsa-miR-34a were represented with the binary code (Fig. 1A).

3.2 Calculation of SNS and DNS Values

To calculate miRNA-miRNA quantum interaction score, the quantum matrix was applied here. Ket alignments of miRNA pairs, for example, miRNA1 and miRNA2, will be loaded into left and lower windows of the matrix by the rule shown in Fig. 1B, respectively. Here, hsa-let-7b and hsa-miR-34a were used as a general sample to demonstrate the calculation of SNS. To calculate SNS, we downloaded the mature miRNA sequence data from miRBase. Then the sequences were transformed to binary data as ket alignments. In addition, hsa-let-7b and hsa-miR-34a was transformed and arranged in parallel (Fig. 1A and 1C). Finally, the SNS value between hsa-let-7b and hsa-miR-34a was calculated by summing up SPs, values of cells on the decreasing diagonal of the matrix (Fig. 1D). Since the matrix represents the entanglement state between the two miRNAs, SNS represents the total quantum state of the loaded miRNA pair. SNS values of hsa-let-7b and hsa-miR-34a were represented using the radar chart (Fig. 2) under various situations, such as different scales of unit (from 3mer to 5mer), different sequence arrangements (parallel or antiparallel) (Fig. 2A), and various relative locations (Fig. 2B). The results suggested that SNS values change according to inner state transition of the miRNA pair (one miRNA, blue; the other miRNA, purple; SP, green). We obtained approximately 40 SNS values for the hsa-let-7b and hsa-miR-34a pair (note: some of them had same value but showed different SP shapes). This indicates that SNS was not constant for hsa-let-7b and hsa-miR-34a.

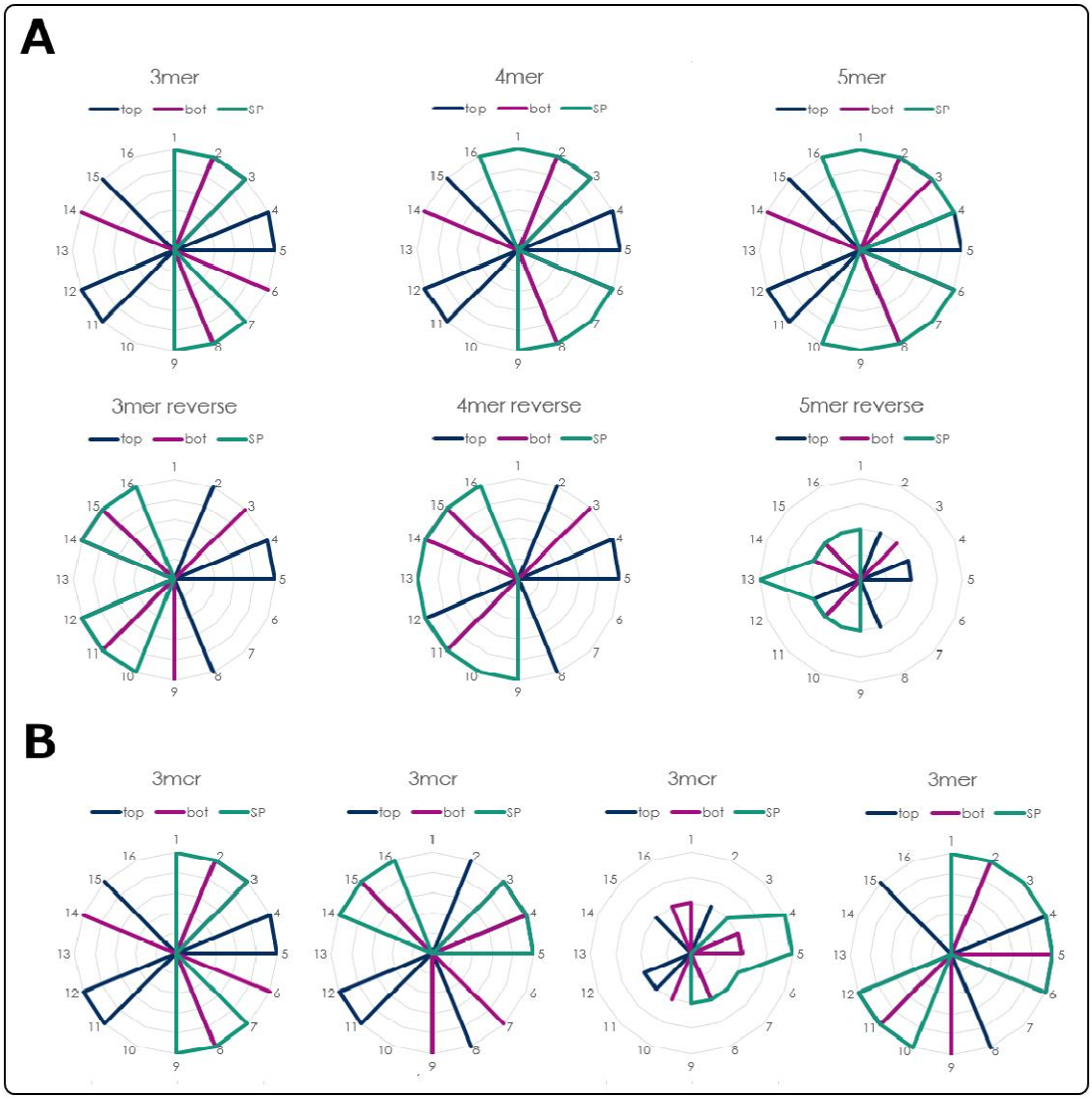

Fig. 2. Transition of SNS value in single miRNA pair

Top: ket alignment of the miRNA on top side. Bot: ket alignment of the mRNA on bottom side. SP: entanglement status between top and bot

To improve the results, we calculated the DNS value using the RNA wave 2000 model, which enables miRNAs to form a torus, and therefore, the relative location of nucleic acid sequences can be shifted. DNS is generated from the sum of all SNS values of the shifted miRNA pairs. DNS was a constant value either after the parallel or antiparallel shifting between the two miRNAs.

3.3 Evaluation of miRNA–miRNA Interactions

Firstly, miRNA ket alignment homology was investigated among 2,588 mature human miRNAs. Complete ket homologies of miRNAs were detected in a total of 107 alignments containing 259 miRNAs, which belong to the same family, subtype, or isomiR. Since 2,426 of 2,588 (93.7%) miRNA kets displayed different individual characteristics, it is obvious that most of miRNA kets are heterogeneous. SNS and DNS values were calculated for different miRNA pairs to evaluate miRNA–miRNA interactions. Human mature miRNA sequences (2,588) were extracted from miRBase, and SNS and DNS general distributions of 3,347,578 miRNA–miRNA pairs were computed. In this experiment, SNS was calculated based on the basic state shown in Fig. 1C. Because all SNS and DNS

values were in multiples of 3, we divided them by 3 in order to draw a graph. Human miRNA SNS values ranged from 0 to 14 and peaked at 1 (Fig. 3A), and human miRNA DNS values ranged from 0 to 288 and peaked at 29 (Fig. 3B). To compare the distributions of SNS and DNS, they were plotted on the same graph, which revealed a much wider range for DNA than for SNS (Fig. 3C). This result indicates that DNS values are more suitable for evaluating miRNA–miRNA interactions. Furthermore, DNS distributions of murine, Drosophila, *Caenorhabditis elegans*, and *Arabidopsis* miRNA–miRNA interactions were investigated individually, and then were compared to each other (Fig. 3D). In murine, Drosophila, *C. elegans*, and *Arabidopsis* species, the maximum values of DNS were 272, 147, 172, and 168, respectively, and DNS peaked at 24 in all species, except for C. elegans (30) (Table 2). Although dominant ranges are similar to each other in all 5 species, proportions of miRNA pairs in dominant range are greatly different. Intriguingly, all of them showed a similar distribution in spite of their various sample sizes (Fig. 4). This indicates that RNA language may be common among plural species.

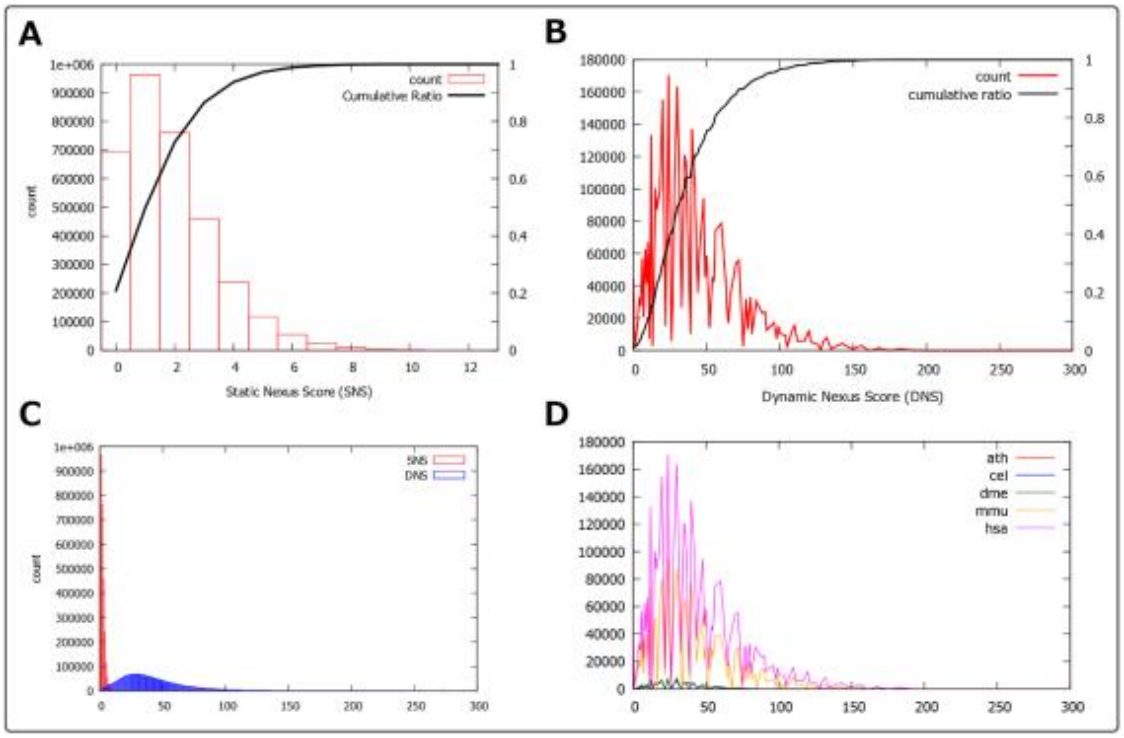

Fig. 3. Contrasts between SNS and DNS, or Human and other species

Table 2. Profiles of miRNA count and DNS distribution in 5 species

Counts of miRNAs	2588 (hsa)	1915 (mmu)	466 (dme)	434 (cel)	427 (ath)
Counts of miRNA pairs	3321753	1832655	108345	93961	90951
Peak DNS value	24	24	24	30	24
(its count)	(170397)	(94858)	(7905)	(6717)	(6150)
Min-max of range	0 – 290	0 – 272	0 – 147	0 – 172	0 – 168
Dominant range of DNS	20 – 40	12 – 40	12 – 40	12 – 42	12 – 42
Counts of miRNA pairs	1291767	941590	68793	67438	63936
included in dominant range	(38.6%)	(51.4%)	(63.5%)	(71.8%)	(70.3%)

Dominant range means the extent between minimum and maximum DNS values which occupy more than 4% count in that of whole DNS

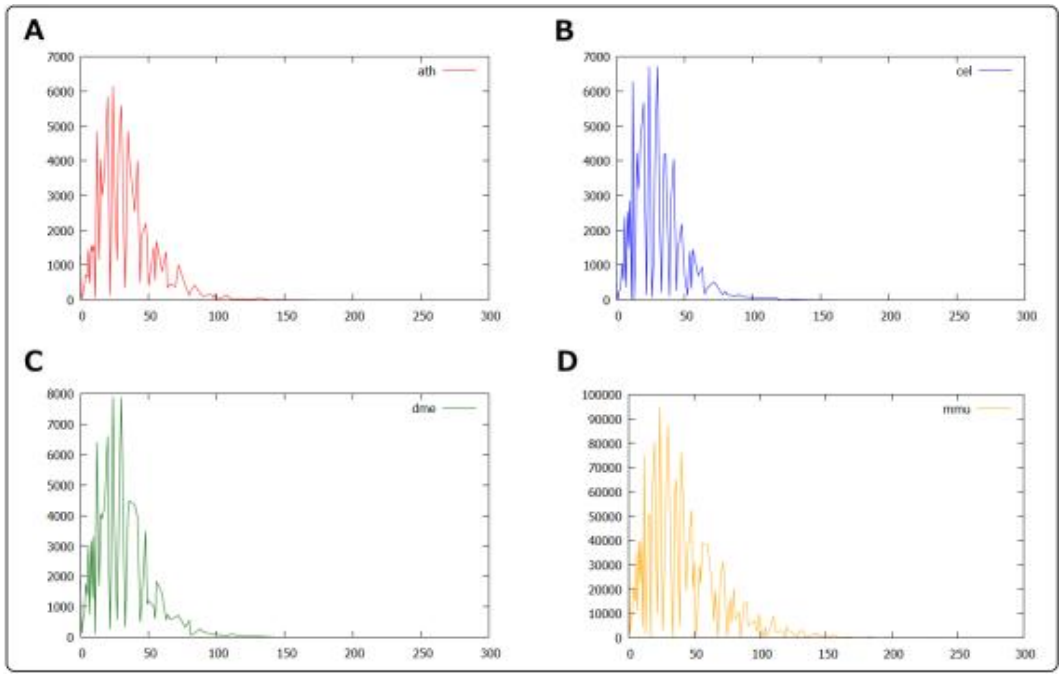

Fig. 4. DNS distributions of 4 different species
X axis: value of DNS, Y axis: count

3.4 Relationship between DNS and SE

We collected scientific papers which report miRNA SEs, then extracted 18 reports that describe about miRNA-miRNA SE. Fifteen reports were related to cancer, 13 of the 18 reports were chosen as samples to examine synergisms between miRNAs (Table 3) [22,27–38]. We built ket alignments of all miRNAs present in these reports, then calculated DNS of these miRNA combinations (Table 4). Finally, the strength of SE for all miRNA pairs were calculated, and 31 DNS and 11 SE values were obtained (Table 5). We observed a positive correlation between 11 of the DNSs and SEs related to malignant diseases (R = 0.55, $P < .06$, $R^2 = 0.2982$) (Fig. 5A). For SNS, 31 data were obtained, but no correlation was observed between SNSs and SEs (Table 6 and Fig. 5B).

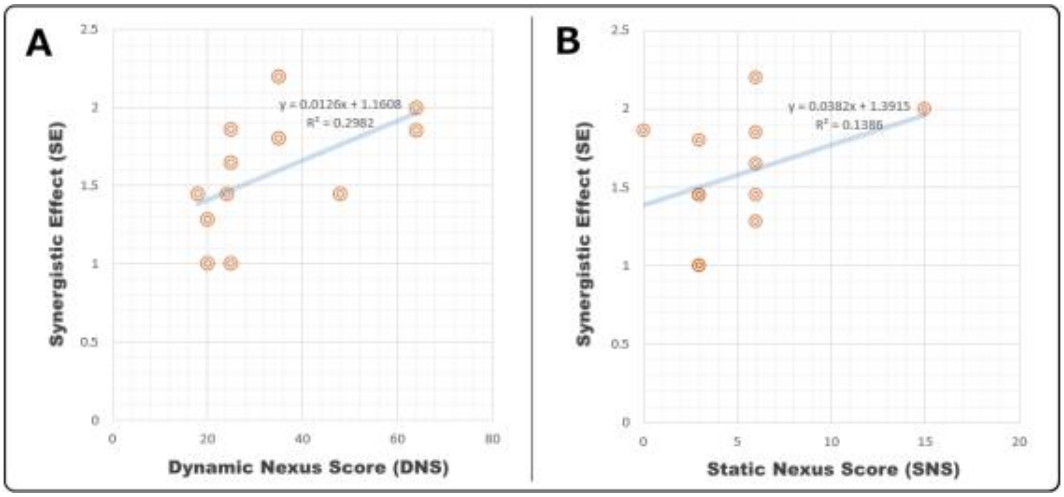

Fig. 5. DNS and SE correlate to each other

Table 3. Synergy-associated miRNA combinations

Biofunctions	Common targets	miRNAs	miRBase ID	Sequences	References
Lung cancer	C-MYC	let-7b-5p	MIMAT0000063	UGAGGUAGUAGGUUGUAUAGUU	[30]
		miR-34a-5p	MIMAT0000255	UGGCAGUGUCUUAGCUGGUUGU	
MDSC induction	SHIP-1	miR-21-5p	MIMAT0000076	UAGCUUAUCAGACUGAUGUUGA	[31]
		miR-155-5p	MIMAT0000646	UUAAUGCUAAUCGUGAUAGGGGU	
proliferation / invasion	MMP-2, EGFR, PDCD4	miR-21-5p	MIMAT0000076	UAGCUUAUCAGACUGAUGUUGA	[32]
		miR-10b-5p	MIMAT0000254	UACCCUGUAGAACCGAAUUUGUG	
colon cancer	-	miR-491-5p	MIMAT0002807	AGUGGGGAACCCUUCCAUGAGG	[33]
		miR-221-3p	MIMAT0000278	AGCUACAUUGUCUGCUGGGUUUC	
		miR-342-3p	MIMAT0000753	UCUCACACAGAAAUCGCACCCGU	
proliferation / survive	WEE1	miR-381-3p	MIMAT0000736	UAUACAAGGGCAAGCUCUCUGU	[34]
		miR-424-5p	MIMAT0001341	CAGCAGCAAUUCAUGUUUUGAA	
cell viability	-	miR-21-5p	MIMAT0000076	UAGCUUAUCAGACUGAUGUUGA	[23]
		miR-1-3p	MIMAT0000416	UGGAAUGUAAAGAAGUAUGUAU	
tumor growth	EphA2	miR-520d-3p	MIMAT0002856	AAAGUGCUUCUCUUUGGUGGGU	[35]
		si-Eph2A-2	(Eph2A: NM_004431.3)	CCAUCAAGAUGCAGCAGUA	
p63 cell cycle	Cyclin D1, E2, CDK4, 6, E2F3, Bcl2, etc.	miR-34a-5p	MIMAT0000255	UGGCAGUGUCUUAGCUGGUUGU	[36]
		miR-34c-5p	MIMAT0000686	AGGCAGUGUAGUUAGCUGAUUGC	
glioma	-	miR-21-5p	MIMAT0000076	UAGCUUAUCAGACUGAUGUUGA	[37]
		miR-23b-5p	MIMAT0004587	UGGGUUCCUGGCAUGCUGAUUU	
		miR-181d-5p	MIMAT0002821	AACAUUCAUUGCUGUCGGUGGGU	
milk fat synthesis	-	miR-23a-3p	MIMAT0000078	AUCACAUUGCCAGGGAUUUCC	[38]
		miR-27b-3p	MIMAT0000419	UUCACAGUGGCUAAGUUCUGC	
		miR-103-3p	MIMAT0000101	AGCAGCAUUGUACAGGGCUAUGA	
		miR-200a-3p	MIMAT0000682	UAACACUGUCUGGUAACGAUGU	
tumor growth	PDCD4	miR-21-5p	MIMAT0000076	UAGCUUAUCAGACUGAUGUUGA	[39]
	BTG2	miR-23a-3p	MIMAT0000078	AUCACAUUGCCAGGGAUUUCC	

Biofunctions	Common targets	miRNAs	miRBase ID	Sequences	References
	NEDD4L	miR-27a-3p	MIMAT0000084	UUCACAGUGGCUAAGUUCCG	
proliferation	-	miR-19b-3p	MIMAT0000074	UGUGCAAAUCCAUGCAAAACUGA	[40]
		miR-21-5p	MIMAT0000076	UAGCUUAUCAGACUGAUGUUGA	
		miR-148a-3p	MIMAT0000243	UCAGUGCACUACAGAACUUUGU	
Carcinoma	E2F5	miR-196a-5p	MIMAT0000226	UAGGUAGUUUCAUGUUGUUGGG	[41]
		miR-337-3p	MIMAT0000754	CUCCUAUAUGAUGCCUUUCUUC	
		let-7c-5p	MIMAT0000064	UGAGGUAGUAGGUUGUAUGGUU	
	MCM4	miR-196a-5p	MIMAT0000226	UAGGUAGUUUCAUGUUGUUGGG	
		miR-337-3p	MIMAT0000754	CUCCUAUAUGAUGCCUUUCUUC	
		miR-99a-3p	MIMAT0004511	CAAGCUCGCUUCUAUGGGUCUG	
	TP53	miR-328-3p	MIMAT0000752	CUGGCCCUCUCUGCCCUUCCGU	
		let-7c-5p	MIMAT0000064	UGAGGUAGUAGGUUGUAUGGUU	
	SKP2	miR-337-3p	MIMAT0000754	CUCCUAUAUGAUGCCUUUCUUC	
		let-7c-5p	MIMAT0000064	UGAGGUAGUAGGUUGUAUGGUU	
	CDK1	miR-196a-5p	MIMAT0000226	UAGGUAGUUUCAUGUUGUUGGG	
		miR-337-3p	MIMAT0000754	CUCCUAUAUGAUGCCUUUCUUC	

Table 4. miRNA kets and its combination and DNS

Biofunctions	miRNAs	Ket alignments	Combinations	DNSs
lung cancer	let-7b	| 010110010011001000010000 >	let-7b / miR-34	64
	miR-34a	| 011001010000010011001000 >		
MDSC induction	miR-21	| 001000000010001001001000 >	miR-21 / miR-155	35
	miR-155	| 000001000000101000111100 >		
Proliferation /	miR-21	| 001000000010001001001000 >	miR-21 / miR-10b	25
invasion	miR-10b	| 000000100100001000001010 >		
Colon cancer	miR-491-5p	| 010111100000000000101100 >	miR-491 / miR-221	48
	miR-221-3p	| 010000000100010011100000 >	miR-491 / miR-342	24
	miR-342-3p	| 000000000100000100000100 >	miR-342 / miR-221	18
Proliferation /	miR-381	| 000000011100010000001000 >	miR-381 / miR-424	25
survive	miR-424	| 001001000000001000010000 >		
Cell viability	miR-21	| 001000000010001001001000 >	miR-21 / miR-1	35
	miR-1	| 011000100001001000100000 >		
Tumor growth	miR-520d-3p	| 000101000000000110111000 >	miR-520d-3p /	35
	Eph2A-siRNA	| 000000010010010010000000 >	siRNA	
p63 cell cycle	miR-34a	| 011001010000010011001000 >	miR-34a / miR-34c	64
	miR-34c	| 011001010010001001000100 >		
Glioma	miR-21	| 001000000010001001001000 >	miR-21 / miR-23b	35
	miR-23b	| 011100000110001001000000 >	miR-21 / miR-181d	35
	miR-181d	| 000000000010010011011100 >	miR-23b / miR-181d	49
Milk fat synthesis	miR-23a	| 000000001000111000000000 >	miR-23a / miR-27b	24
	miR-27b-3p	| 000000101100001000010000 >	miR-103 / miR-200a	35
	miR-103-3p	| 010010000100001110000100 >	miR-27b / miR-200a	40
	miR-200a	| 000000010001100001001000 >		
Tumor growth	miR-21	| 001000000010001001001000 >	miR-21 / miR-23a	20
	miR-23a-3p	| 000000001000111000000000 >	miR-21 / miR-27a	25
	miR-27a-3p	| 000000101100001000010000 >	miR-23a / miR-27a	20
proliferation	miR-19b-3p	| 010100000000010000000100 >	miR-19b / miR-21	20
	miR-21	| 001000000010001001001000 >	miR-19b / miR-148a	16
	miR-148a	| 000101000000010000001000 >	miR-21 / miR-148a	20
Carcinoma	miR-196a-5p	| 001100100000010010011100 >	miR-196a / miR-337	16
	miR-337-3p	| 000000000100100000000000 >	miR-196a / let-7c	72
	let-7c-5p	| 010110010011001000110000 >	let-7c / miR-337	18
	miR-196a-5p	| 001100100000010010011100 >	miR-196a / miR-99a	48
	miR-337-3p	| 000000000100100000000000 >	miR-337 / miR-99a	12
	miR-99a-3p	| 000100010000000111000100 >	miR-196a / miR-337	16
	miR-328-3p	| 001100000000100000001000 >	miR-328 / let-7c	36
	let-7c-5p	| 010110010011001000110000 >		
	miR-337-3p	| 000000000100100000000000 >	miR-337 / let-7c	18
	let-7c-5p	| 010110010011001000110000 >		
	miR-196a-5p	| 001100100000010010011100 >	miR-196a / miR-337	16
	miR-337-3p	| 000000000100100000000000 >		

4. DISCUSSION

There is an increasing need for the prediction of miRNA function and synergy. Many current studies explore miRNA targets using computing methods, and similarly, these approaches are used for detecting novel miRNAs and predicting miRNA functions or synergisms. These methods are based on the mRNA–miRNA interaction theory and various miRNA target databases (Table 1) [15,16]. TargetScan, miRanda, and miRDB are the most frequently used miRNA target prediction tools, and they are primarily based on sequence complementarity, and thus binding strength and stability between the mRNA target site and the miRNA or its seed region [14,42,43]. DIANA-microT, PicTar, and RNAhybrid are other common miRNA target prediction tools, but they are based on thermodynamic data of the mRNA–miRNA complex such as stability and free energy state [17,18,42-44]. Ordinarily, differential theory-based algorithms are used in combination to improve the precision of predictions [45,46].

Table 5. DNS values and SE strengths

Biofunctions	Combinations	DNSs	SEs
lung cancer	let-7b / miR-34a	64	1.85
MDSC induction	miR-21 / miR-155	35	NA
proliferation / invasion	miR-21 / miR-10b	25	1.65
colon cancer	miR-491 / miR-221	48	1.45
colon cancer	miR-491 / miR-342	24	1.45
colon cancer	miR-342 / miR-221	18	1.45
proliferation / survive	miR-381 / miR-424	25	1.86
cell viability	miR-21 / miR-1	35	2.2
tumor growth	miR-520d-3p / siRNA	35	1.8
p63 cell cycle	miR-34a / miR-34c	64	2
glioma	miR-21 / miR-23b	35	NA
glioma	miR-21 / miR-181d	35	NA
glioma	miR-23b / miR-181d	49	NA
milk fat synthesis	miR-23a / miR-27b	24	NA
milk fat synthesis	miR-103 / miR-200a	35	NA
milk fat synthesis	miR-27b / miR-200a	30	NA
tumor growth	miR-21 / miR-23a	20	1
tumor growth	miR-21 / miR-27a	25	1
tumor growth	miR-23a / miR-27a	20	1.28
proliferation	miR-19b / miR-21	20	NA
proliferation	miR-19b / miR-148a	16	NA
proliferation	miR-21 / miR-148a	20	NA
Carcinoma	miR-196a / miR-337	16	NA
Carcinoma	miR-196a / let-7c	72	NA
Carcinoma	let-7c / miR-337	18	NA
Carcinoma	miR-196a / miR-99a	48	NA
Carcinoma	miR-337 / miR-99a	12	NA
Carcinoma	miR-196a / miR-337	16	NA
Carcinoma	miR-328 / let-7c	36	NA
Carcinoma	miR-337 / let-7c	18	NA
Carcinoma	miR-196a / miR-337	48	NA

NA means that any synergistic effect was not obtained as specific value

Although these computational techniques have been improved and now produce more accurate results, false positive results are still obtained. Prediction algorithms have a technical limitation whereby it is difficult to improve prediction accuracy by regarding only complementarity, homology, and thermodynamics. Therefore, novel approaches are necessary to improve and calibrate prediction algorithms.

To improve the accuracy of miRNA target and synergy prediction algorithms, contribution of new factors, such as miRNA clusters, conservations, and transcription start sites (TSSs), are now considered [7,47–49]. MicroTSS integrates RNA sequence data, active transcription marks, and DNase I hypersensitive site sequencing results, and this concept enabled the identification of various tissue-specific pri-miRNAs and intergenic miRNAs [49]. Furthermore, miRNAs can interact with themselves, for example, via miRNA–miRNA bindings [50,51]. Certain miRNAs form homologous or heterologous miRNA pairs, which suggests that miRNA synergism is caused not only by co-expression and co-target relationships but also by direct interactions. We also tried to add novel factors to generate a more accurate computation method by adopting the RNA wave 2000 model, which includes numerous new factors, such as quantum energy, torus, miRNA pairs, and G potential.

Among the four types of nucleotides, G is the only one that has a positive FMO-electric charge [24]. This specific characteristic is linked to certain clinical and technical aspects. G is a prominent target for mutations in cancer and inherited diseases [52], and G quartets enable the ultrasensitive detection of miRNAs [53]. Additionally, G bases may have unknown roles in gene regulation, and they may be a critical factor

Table 6. SNS values and SE strengths

Biofunctions	Combinations	SNSs	SEs
lung cancer	let-7b / miR-34a	2	1.85
MDSC induction	miR-21 / miR-155	2	NA
oncogene	miR-21 / miR-10b	2	1.65
colon cancer	miR-491 / miR-221	2	1.45
colon cancer	miR-491 / miR-342	1	1.45
colon cancer	miR-342 / miR-221	1	1.45
proliferation / survive	miR-381 / miR-424	0	1.86
cell viability	miR-21 / miR-1	2	2.2
tumor growth	miR-520d-3p / siRNA	1	1.8
p63 cell cycle	miR-34a / miR-34c	5	2
glioma	miR-21 / miR-23b	4	NA
glioma	miR-21 / miR-181d	3	NA
glioma	miR-23b / miR-181d	2	NA
milk fat synthesis	miR-23a / miR-27b	2	NA
milk fat synthesis	miR-103 / miR-200a	0	NA
milk fat synthesis	miR-27b / miR-200a	0	NA
tumor growth	miR-21 / miR-23a	1	1
tumor growth	miR-21 / miR-27a	1	1
tumor growth	miR-23a / miR-27a	2	1.28
proliferation	miR-19b / miR-21	0	NA
proliferation	miR-19b / miR-148a	2	NA
proliferation	miR-21 / miR-148a	1	NA
Carcinoma	miR-196a / miR-337	0	NA
Carcinoma	miR-196a / let-7c	2	NA
Carcinoma	let-7c / miR-337	0	NA
Carcinoma	miR-196a / miR-99a	3	NA
Carcinoma	miR-337 / miR-99a	0	NA
Carcinoma	miR-196a / miR-337	0	NA
Carcinoma	miR-328 / let-7c	1	NA
Carcinoma	miR-337 / let-7c	0	NA
Carcinoma	miR-196a / miR-337	0	NA

for the *bona fide* construction of miRNA–miRNA, mRNA–miRNA, or DNA–miRNA interaction models [54].

Preliminarily, we examined the context + score values of all co-target genes present in Table 3 using TargetScan. Only 3 mRNAs, RAS, CDK, and Rho were found, and their context+ score value was −0.35 (let-7b), −0.25 (miR-491), and −0.22 (miR-21), respectively. Curiously, DNS of let-7b/miR-34a, miR-491/miR-221, and miR-21/miR-10b, is 64, 48, and 25, respectively; therefore, these context+ scores were directly proportional to the DNS values, even though the context + score is based on mRNA–miRNA interactions and DNS is based on miRNA–miRNA interactions. This implies that miRNA synergism and mRNA targeting may be coupled. Context+ score is associated with human diseases according to the polymiRTS database [55], and miRNA-related single nucleotide polymorphisms are scored by the context+ score. Therefore, further investigations using DNS are crucial for building an integrated model of miRNA–miRNA interactions as miRNA memory device and to identify mRNA–miRNA interactions based on human disease databases.

5. CONCLUSION

In our analysis, we could utilize only a very limited sample size because there are still few reports about miRNA synergisms. However, we found a synergistic effect in miRNA–miRNA interactions from the perspective of quantum energy as miRNA memory. We suggest that more precise cancer-related prediction could be achieved using specific G-based DNS analysis in addition to conventional mRNA-miRNA interaction factors such as thermodynamic stability.

CONSENT

It is not applicable.

ETHICAL APPROVAL

It is not applicable.

COMPETING INTERESTS

Authors have declared that no competing interests exist.

REFERENCES

1. David B. MicroRNAs: Genomics, biogenesis, mechanism, and function. Cell. 2004;116:281–297.
2. Kim VN, Han J, Siomi MC. Biogenesis of small RNAs in animals. Nat Rev Mol Cell Biol. 2009;10:126–139.
3. Grey F, Tirabassi R, Meyers H, Wu G, McWeeney S, Hook L, Nelson JA. A viral microRNA down-regulates multiple cell cycle genes through mRNA 5′UTRs. PLoS Pathog. 2010;6(6):e1000967.
4. Xu L, Dai WQ, Xu XF, Wang F, He L, Guo CY. Effects of multiple-target anti-microRNA antisense Oligodeoxyribonucleotides on proliferation and migration of gastric cancer cells. Asian Pacific J Cancer Prev. 2012;13:3203–3207.
5. Gama-Carvalho M, Andrade J, Brás-Rosário L. Regulation of cardiac cell fate by microRNAs: Implications for heart regeneration. Cells. 2014;3:996–1026.
6. Fujii YR. Oncoviruses and pathogenic MicroRNAs in humans. Open Virol J. 2009; 3:37–51.
7. Lewis BP, Burge CB, Bartel DP. Conserved seed pairing, often flanked by adenosines, indicates that thousands of human genes are MicroRNA targets. Cell. 2005;120:15–20.
8. La Rocca G, Olejniczak SH, González AJ, Briskin D, Vidigal Ja, Spraggon L, DeMatteo RG, Radler MR, Lindsten T, Ventura A, Tuschl T, Leslie CS, Thompson CB. *In vivo*, Argonaute-bound microRNAs exist predominantly in a reservoir of low molecular weight complexes not associated with mRNA. Proc Natl Acad Sci. 2015;112:767–772.
9. Pinder BD, Smibert CA. Smaug: An unexpected journey into the mechanisms of post-transcriptional regulation. Fly (Austin); 2013.
   DOI: 10.4161/fly.24336
10. Srikantan S, Marasa BS, Becker KG, Gorospe M, Abdelmohsen K. Paradoxical microRNAs: Individual gene repressors, global translation enhancers. Cell Cycle. 2011;10:751–759.
11. Laganà A, Acunzo M, Romano G, Pulvirenti A, Veneziano D, Cascione L, Giugno R, Gasparini P, Shasha D, Ferro A, Croce CM. MiR-Synth: A computational resource for the design of multi-site multi-target synthetic miRNAs. Nucleic Acids Res. 2014;42:5416–5425.
12. Meng Q-W, Zhang Z-P, Wang W, Tian J, Xiao Z-G. Enhanced inhibition of *Avian leukosis virus* subgroup J replication by multi-target miRNAs. Virol J. 2011;8:556.
13. Heikham R, Shankar R. Flanking region sequence information to refine microRNA target predictions. J Biosci. 2010;35:105–118.
14. Wong N, Wang X. miRDB: An online resource for microRNA target prediction and functional annotations. Nucleic Acids Res. 2014;43:D146–D152.
15. Mazière P, Enright AJ. Prediction of microRNA targets. Drug Discov Today. 2007;12:452-458.
16. Ekimler S, Sahin K. Computational methods for MicroRNA target prediction. Genes (Basel). 2014;5:671–683.
17. Paraskevopoulou MD, Georgakilas G, Kostoulas N, Vlachos IS, Vergoulis T, Reczko M, Filippidis C, Dalamagas T, Hatzigeorgiou AG. DIANA-microT web server v5.0: Service integration into miRNA functional analysis workflows. Nucleic Acids Res. 2013;41:W169–W173.
18. Krüger J, Rehmsmeier M. RNAhybrid: MicroRNA target prediction easy, fast and flexible. Nucleic Acids Res. 2006; 34:W451–W454.
19. Ding J, Li X, Hu H. MicroRNA modules prefer to bind weak and unconventional target sites. Bioinformatics. 2015;31(9): 1366-1374.
20. Xu J, Li CX, Li YS, Lv JY, Ma Y, Shao TT, Xu L De, Wang YY, Du L, Zhang YP, Jiang W, Li CQ, Xiao Y, Li X. MiRNA-miRNA synergistic network: Construction via co-regulating functional modules and disease miRNA topological features. Nucleic Acids Res. 2011;39:825–836.
21. Dimitrakopoulou K, Vrahatis AG, Bezerianos A. Integromics network meta-analysis on cardiac aging offers robust multi-layer modular signatures and reveals micronome synergism. BMC Genomics. 2015;16:147.
22. Morozova N, Nonne N, Pritchard L-L, Harel-Bellan a, Morozova N, Nonne N,

Pritchard L-L, Harel-Bellan a, Zinovyev a, Zinovyev a, Zinovyev a, Gorban A: Kinetic signatures of microRNA modes of action. RNA. 2012;18:1635–1655.
23. Zhu W, Zhao Y, Xu Y, Sun Y, Wang Z, Yuan W, Du Z. Dissection of protein interactomics highlights MicroRNA synergy. PLoS One. 2013;8(5):e63342
24. Fujii YR. The RNA gene information: retroelement-MicroRNA entangling as the RNA quantum code. In: Ying S-Y, editors: MicroRNA Protocols. 2nd ed. Life Sci. 2013; 47-67.
25. Fujii YR. Formulation of new algorithmics for miRNAs. Open Virol J. 2008;2:37–43.
26. Fujii YR. RNA wave for the HIV therapy : Foods, stem cells and the RNA information gene. World J AIDS. 2013;3:131–146.
27. Kozomara A, Griffiths-Jones S. MiRBase: Annotating high confidence microRNAs using deep sequencing data. Nucleic Acids Res. 2014;42:68–73.
28. Calderbank aR, Rains EM, Shor PW, Sloane NJA. Quantum error correction and orthogonal geometry. Phys. Rev. Lett. 1996;78:405-408.
29. Fujii YR, Osone T, Yoshikawa M. MESer; 2014.
Available:http://meser.mirna-academy.org/
(Accessed 28 May 2015)
30. Kasinski aL, Kelnar K, Stahlhut C, Orellana E, Zhao J, Shimer E, Dysart S, Chen X, Bader aG, Slack FJ. A combinatorial microRNA therapeutics approach to suppressing non-small cell lung cancer. Oncogene. 2014;34:3547-3555.
31. Li L, Zhang J, Diao W, Wang D, Wei Y, Zhang C-Y, Zen K. MicroRNA-155 and MicroRNA-21 promote the expansion of functional myeloid-derived suppressor cells. J Immunol. 2014;192:1034-1043.
32. Dong CG, Wu WKK, Feng SY, Wang XJ, Shao JF, Qiao J. Co-inhibition of microRNA-10b and microRNA-21 exerts synergistic inhibition on the proliferation and invasion of human glioma cells. Int J Oncol. 2012;41:1005–1012.
33. Tao K, Yang J, Guo Z, Hu Y, Sheng H, Gao H, Yu H. Prognostic value of miR-221-3p, miR-342-3p and miR-491-5p expression in colon cancer. Am J Transl Res. 2014; 6:391–401.
34. Chen B, Duan L, Yin G, Tan J, Jiang X. Simultaneously expressed miR-424 and miR-381 synergistically suppress the proliferation and survival of renal cancer cells---Cdc2 activity is up-regulated by targeting WEE1. Clinics. 2013;68:825–833.
35. Nishimura M, Jung EJ, Shah MY, Lu C, Spizzo R, Shimizu M, Han HD, Ivan C, Rossi S, Zhang X, Nicoloso MS, Wu SY, Almeida MI, Bottsford-Miller J, Pecot CV, Zand B, Matsuo K, Shahzad MM, Jennings NB, Rodriguez-Aguayo C, Lopez-Berestein G, Sood AK, Calin GA. Therapeutic synergy between microRNA and siRNA in ovarian cancer treatment. Cancer Discov. 2013;3:1302–1315.
36. Antonini D, Russo MT, De Rosa L, Gorrese M, Del Vecchio L, Missero C. Transcriptional repression of miR-34 family contributes to p63-mediated cell cycle progression in epidermal cells. J Invest Dermatol. 2010;130:1249–1257.
37. Li R, Li X, Ning S, Ye J, Han L, Kang C, Li X. Identification of a core miRNA-pathway regulatory network in glioma by therapeutically targeting miR-181d, miR-21, miR-23b, β-Catenin, CBP, and STAT3. PLoS One. 2014;9(7):e101903.
38. Lin X, Luo J, Zhang L, Zhu J. MicroRNAs synergistically regulate milk fat synthesis in mammary gland epithelial cells of dairy goats. Gene Expr. 2013;16:1–13.
39. Frampton AE, Castellano L, Colombo T, Giovannetti E, Krell J, Jacob J, Pellegrino L, Roca-Alonso L, Funel N, Gall TMH, De Giorgio A, Pinho FG, Fulci V, Britton DJ, Ahmad R, Habib N a, Coombes RC, Harding V, Knösel T, Stebbing J, Jiao LR. MicroRNAs cooperatively inhibit a network of tumor suppressor genes to promote pancreatic tumor growth and progression. Gastroenterology. 2014;146:268–277.
40. Wang P, Phan T, Gordon D, Chung S, Henning SM, Vadgama JV. Arctigenin in combination with quercetin synergistically enhances the antiproliferative effect in prostate cancer cells. Mol Nutr Food Res. 2015;59:250–261.
41. Xiong H, Li Q, Liu S, Wang F, Xiong Z, Chen J, Chen H, Yang Y, Tan X, Luo Q, Peng J, Xiao G, Jiang Q. Integrated microRNA and mRNA transcriptome sequencing reveals the potential roles of miRNAs in stage I endometrioid endometrial carcinoma. PLoS One. 2014; 9(10):e110163.
42. Lewis BP, Shih IH, Jones-Rhoades MW, Bartel DP, Burge CB. Prediction of mammalian MicroRNA targets. Cell. 2003; 115:787–798.
43. Wuchty S, Fontana W, Hofacker IL, Schuster P. Complete suboptimal folding of

RNA and the stability of secondary structures. Biopolymers. 1999;49:145–165.

44. Hofacker IL. How microRNAs choose their targets. Nat Genet. 2007;39:1191–1192.
45. Krek A, Grün D, Poy MN, Wolf R, Rosenberg L, Epstein EJ, MacMenamin P, da Piedade I, Gunsalus KC, Stoffel M, Rajewsky N. Combinatorial microRNA target predictions. Nat Genet. 2005;37: 495-500
46. Kiriakidou M, Nelson PT, Kouranov A, Fitziev P, Bouyioukos C, Mourelatos Z, Hatzigeorgiou A. A combined computational-experimental approach predicts human microRNA targets. Genes Dev. 2004;18:1165–1178.
47. Leung W-S, Lin MCM, Cheung DW, Yiu SM: Filtering of false positive microRNA candidates by a clustering-based approach. BMC Bioinformatics. 2008;9(Suppl 12):S3.
48. Marin RM, Vanicek J. Optimal use of conservation and accessibility filters in MicroRNA target prediction. PLoS One. 2012;7(2):e32208
49. Georgakilas G, Vlachos IS, Paraskevopoulou MD, Yang P, Zhang Y, Economides AN, Hatzigeorgiou AG. microTSS: Accurate microRNA transcriptional start site indetification reveals a significant number of divergent pri-miRNAs. Nat Commun. 2014;5:5700.
50. Lai EC, Wiel C, Rubin GM. Complementary miRNA pairs suggest a regulatory role for miRNA:miRNA duplexes. RNA. 2004;10:171–175.
51. Maiti M, Nauwelaerts K, Lescrinier E, Schuit FC, Herdewijn P. Self-complementary sequence context in mature miRNAs. Biochem Biophys Res Commun. 2010;392:572–576.
52. Bacolla A, Temiz Na, Yi M, Ivanic J, Cer RZ, Donohue DE, Ball E V., Mudunuri US, Wang G, Jain A, Volfovsky N, Luke BT, Stephens RM, Cooper DN, Collins JR, Vasquez KM. Guanine holes are prominent targets for mutation in cancer and inherited disease. PLoS Genet. 2013;9(9):e1003816.
53. Yan L, Yan Y, Pei L, Wei W, Zhao J. A G-quadruplex DNA-based, label-free and ultrasensitive strategy for microRNA detection. Sci Rep. 2014;4:7400.
54. Koo CX, Kobiyama K, Shen YJ, LeBert N, Ahmad S, Khatoo M, Aoshi T, Gasser S, Ishii KJ. RNA polymerase iii regulates cytosolic RNA: DNA hybrids and intracellular MicroRNA expression. J Biol Chem. 2015;290:7463-7473.
55. Bhattacharya A, Ziebarth JD, Cui Y. PolymiRTS Database 3.0: Linking polymorphisms in microRNAs and their target sites with human diseases and biological pathways. Nucleic Acids Res. 2014;42:D86–D91.

Peer-review history:
The peer review history for this paper can be accessed here:
http://sciencedomain.org/review-history/12414